Oxidatively induced Alkyne Rotation in Dicobalt Complexes: Structural Tests of Molecular Orbital Theory *

R. Paul Aggarwal, Neil G. Connelly, M. Carmen Crespo, Barry J. Dunne, Philippa M. Hopkins and A. Guy Orpen
School of Chemistry, University of Bristol, Bristol BS8 1TS, UK

The complexes $[Co_2(CO)_2(\mu\text{-}RC_2R)(\mu\text{-}dppm)_2]$ **1** (R = Me, Ph or CO_2Me; dppm = $Ph_2PCH_2PPh_2$) undergo reversible one-electron oxidation at a platinum-bead electrode in CH_2Cl_2; chemical oxidation of **1** with the ferrocenium ion or with iodine gives stable salts of the monocations $\mathbf{1}^+$. The X-ray structures of **1** (R = Me and Ph) show the alkyne bridge to be orthogonal to a cobalt–cobalt bond which is also bridged by the two dppm ligands. The overall structure of $\mathbf{1}^+$ (R = Me), as its $[PF_6]^-$ salt, is similar but with the alkyne bridge rotated by 12° about an axis perpendicular to the shortened metal–metal bond. The structural changes observed provide direct experimental support for previous bonding studies of the structural preferences of hydrocarbon-bridged $M_2(CO)_6$ complexes.

As a part of a wider theoretical study of the general class of compounds containing hydrocarbons bound to $M_2(CO)_6$ centres Thorn and Hoffmann[1] used extended-Hückel molecular orbital (EHMO) methods to predict that the replacement of cobalt in $[Co_2(CO)_6(\mu\text{-}RC_2R)]$ by iron (*i.e.* loss of two electrons from the 34 valence electron dimetal species) should result in a rotation of the alkyne with respect to the metal–metal vector of *ca.* 20–30°; a similar rotation was independently predicted by Anderson.[2] In fact, however, $[Fe_2(CO)_6(\mu\text{-}Bu^tC_2Bu^t)]$, the only structurally characterised[3] species of the type $[Fe_2(CO)_6(\mu\text{-}RC_2R)]$, shows little or no such rotation (*ca.* 5°). Instead, there is a second distortion involving a relative twisting of the two $Fe(CO)_3$ groups to give a staggered $Fe_2(CO)_6$ conformation rather than the eclipsed geometry inevitably found in $[Co_2(CO)_6(\mu\text{-}RC_2R)]$ and its carbonyl substitution products.[4]

We now provide details[5] of synthetic, structural and electrochemical studies which provide the first direct experimental confirmation of the correctness of Thorn and Hoffmann's predictions. Thus, we describe the synthesis of $[Co_2(CO)_2(\mu\text{-}RC_2R)(\mu\text{-}dppm)_2]$ (R = Me, Ph or CO_2Me; dppm = $Ph_2PCH_2PPh_2$) species where the relative geometry of the two $Co(CO)L_2$ units is constrained to be eclipsed, and structural comparisons of the redox pair $[Co_2(CO)_2(\mu\text{-}MeC_2Me)(\mu\text{-}dppm)_2]$ and $[Co_2(CO)_2(\mu\text{-}MeC_2Me)(\mu\text{-}dppm)_2]^+$ and the phenyl-substituted analogue $[Co_2(CO)_2(\mu\text{-}PhC_2Ph)(\mu\text{-}dppm)_2]$ which confirm that one-electron oxidation of $[Co_2(CO)_2(\mu\text{-}RC_2R)(\mu\text{-}dppm)_2]$ results in just the alkyne rotation predicted. Taken with previous ESR spectroscopic studies[6] of the anions $[Co_2(CO)_6(\mu\text{-}RC_2R)]^-$, the present work provides a detailed description of the bonding in $[M_2(CO)_6(\mu\text{-}RC_2R)]$ and in particular the effects of one-electron removal from the highest occupied molecular orbital (HOMO), and one-electron addition to the lowest unoccupied molecular orbital (LUMO) of $[Co_2(CO)_6(\mu\text{-}RC_2R)]$ and analogous species.

Results and Discussion

Synthesis and Electrochemistry of $[Co_2(CO)_2(\mu\text{-}RC_2R)(\mu\text{-}dppm)_2]$.—The complexes $[Co_2(CO)_2(\mu\text{-}RC_2R)(\mu\text{-}dppm)_2]$ **1** were isolated as air-stable dark red to purple crystals either directly from $[Co_2(CO)_6(\mu\text{-}RC_2R)]$ and 2 equivalents of dppm in refluxing toluene [**1** (R = Ph)] or stepwise by first preparing $[Co_2(CO)_4(\mu\text{-}RC_2R)(\mu\text{-}dppm)]$ from $[Co_2(CO)_6(\mu\text{-}RC_2R)]$ and 1 equivalent of dppm in hexane, and then treating it [**1** (R = Me or CO_2Me)], with a second equivalent of dppm, again in refluxing toluene; similar methods have been used previously to synthesise the closely related ditertiary arsine derivative $[Co_2(CO)_2(\mu\text{-}RC_2R)(\mu\text{-}dpam)_2]$ (dpam = $Ph_2AsCH_2AsPh_2$)[7] and $[Co_2(CO)_2(\mu\text{-}RC_2R)\{P(OMe)_3\}_4]$ (R = Ph or CF_3).[8] After purification from CH_2Cl_2–hexane [**1** (R = Ph)] or CH_2Cl_2–methanol [**1** (R = Me or CO_2Me)] the complexes were characterised by elemental analysis (Table 1) [**1** (R = Ph) and **1** (R = CO_2Me) as 1:1 and 2:1 CH_2Cl_2 solvates respectively (confirmed by ^1H NMR spectroscopy in $CDCl_3$)] and by their IR carbonyl spectra each of which showed one absorption at *ca.* 1900–1940 cm^{-1}. In the case of **1** (R = Ph) the ^{31}P NMR spectrum (20% CD_2Cl_2 in CH_2Cl_2) showed only one singlet (δ 39.5) as expected for a symmetric structure in which the alkyne and two dppm ligands symmetrically bridge the $Co_2(CO)_2$ core {*i.e.* in a structure closely related to that of $[Co_2(CO)_6(\mu\text{-}RC_2R)]$}.

In CH_2Cl_2, at a platinum electrode, the cyclic voltammogram of each of the dicarbonyls **1** showed two sequential oxidation waves (Table 1) the first of which is fully reversible $[(i_p)_{red}/(i_p)_{ox} = 1.0$ for scan rates, v, between 50 and 500 mV $s^{-1}]$ and diffusion controlled $[(i_p)_{ox}/v^{\frac{1}{2}} =$ constant]. The second wave, of approximately equal height to the first, is partially chemically reversible. For example, the peak current ratio, $(i_p)_{red}/(i_p)_{ox}$, for the second oxidation of $[Co_2(CO)_2(\mu\text{-}RC_2R)(\mu\text{-}dppm)_2]$ **1** (R = Ph) reaches 1.0 at a scan rate of 1.0 V s^{-1} {suggesting some stability for the dication $[Co_2(CO)_2(\mu\text{-}PhC_2Ph)(\mu\text{-}dppm)_2]^{2+}$ which is isoelectronic with $[Fe_2(CO)_6(\mu\text{-}RC_2R)]$}.

The difference in potential, ΔE, between the two oxidation waves for each of the complexes **1** is approximately 1.0 V, considerably greater than the difference between the potentials for the two oxidation waves of other alkyne-bridged species such as $[Mo_2(CO)_3L(\mu\text{-}RC_2R)(\eta\text{-}C_5R'_5)_2]$ (L = CO or isocyanide; R = Me, CO_2Me, *etc.*; R′ = H, Me, *etc.*)[9] and $[Pd_2(\mu\text{-}PhC_2Ph)(\eta\text{-}C_5Ph_5)_2]$[10] ($\Delta E$ *ca.* 0.5 and 0.61 V respectively). This may reflect the greater stabilisation of the HOMO of **1** on one-electron oxidation when compared with those of the molybdenum and palladium analogues.

The oxidation potential of the first wave (and of the second) depends on the alkyne substituent R in the expected way in that

* *Supplementary data available:* see Instructions for Authors, *J. Chem. Soc., Dalton Trans.*, 1992, Issue 1, pp. xx–xxv.

Non-SI unit employed: G = 154 T.

Table 1 Analytical, spectroscopic and electrochemical[a] data for $[Co_2(CO)_2(\mu\text{-}RC_2R)(\mu\text{-}dppm)_2][X]$

R	X^-	Yield (%)	Colour	Analysis (%)[b] C	H	IR[c] ν(CO)/cm^{-1}	ESR[d] g value	E°[e]/V
Me	—	56	Crimson	67.5 (67.4)	5.1 (5.2)	1896	—	−0.09 (0.95)
Me	PF_6	79	Brown	55.5 (55.8)[f]	4.5 (4.2)	1965	2.11	−0.09 (0.90)
Ph	—	42	Dark purple	66.3 (66.7)[g]	4.8 (4.7)	1923	—	0.09 (0.99)
Ph	PF_6	74	Brown-violet	62.0 (62.6)	4.4 (4.3)	1977	2.12	0.09 (0.97)
Ph	BPh_4	78	Brown	75.0 (75.1)	5.5 (5.1)	1977	*h*	*h*
Ph	I_3	69	Dark purple-violet	52.9 (52.8)	3.8 (3.6)	1977	*h*	*h*
CO_2Me	—	63	Red	62.8 (62.8)[i]	4.7 (4.6)	1942 (1685)	—	0.38 (1.40)
CO_2Me	PF_6	73	Brown	56.9 (56.6)	4.5 (4.1)	2000 (1714)	2.12	0.38 (1.34)

[a] In CH_2Cl_2 at a platinum-bead electrode. Under the conditions used the potentials for the couples $[Fe(\eta\text{-}C_5H_5)_2]^+$–$[Fe(\eta\text{-}C_5H_5)_2]$ and $[Fe(\eta\text{-}C_5Me_5)_2]^+$–$[Fe(\eta\text{-}C_5Me_5)_2]$ are 0.47 and −0.09 V respectively. [b] Calculated values in parentheses. [c] In CH_2Cl_2, ketonic carbonyl in parentheses. [d] At room temperature, in thf–CH_2Cl_2 (2:1). [e] For the first reversible wave, with, in parentheses, the oxidation peak potential, $(E_p)_{ox}$, at a scan rate of 200 mV s^{-1} for the second, irreversible wave. [f] Calculated for a 1:1 CH_2Cl_2 solvate (confirmed by ^1H NMR spectroscopy). [g] Calculated for a 1:1 CH_2Cl_2 solvate (confirmed by X-ray structural analysis). [h] Not measured. [i] Calculated for a 0.5 CH_2Cl_2 solvate.

the most electron-withdrawing group (R = CO_2Me) gives rise to the most positive value of E° (Table 1). The redox potentials also depend on the extent of carbonyl substitution so that $[Co_2(CO)_4(\mu\text{-}PhC_2Ph)(\mu\text{-}dppm)]$ shows two oxidation waves at 0.61 and 1.48 V {*cf.* 0.09 and 0.99 V for $[Co_2(CO)_2(\mu\text{-}RC_2R)(\mu\text{-}dppm)_2]$}. For this tetracarbonyl complex the second cyclic voltammetric wave shows no peak on the reverse scan at scan rates up to 1.0 V s^{-1} (*i.e.* the oxidation process is completely irreversible). Moreover its height is some 2.5 times that of the first wave suggesting a multielectron decomposition process.

The controlled-potential electrolysis of **1** (R = Ph) in CH_2Cl_2, at a platinum-basket electrode ($E_{applied}$ = 0.4 V, 20 min), resulted in the passage of 0.9 F mol^{-1} and the formation of a dark brown solution, the cyclic and rotating-platinum-electrode voltammograms of which showed the quantitative formation of $\mathbf{1}^+$ (R = Ph); one *reduction* wave was observed at a potential identical to that for the oxidation of **1** (R = Ph) and an oxidation wave corresponding to the second oxidation of **1** (R = Ph) was also apparent.

The chemical oxidation of complex **1** was also readily effected using mild one-electron oxidants. For example, treatment of **1** with $[Fe(\eta\text{-}C_5H_5)_2]X$ (X = BF_4, PF_6 or BPh_4) in CH_2Cl_2 gave dark brown solutions from which the salts $[Co_2(CO)_2(\mu\text{-}RC_2R)(\mu\text{-}dppm)_2]X$ $\mathbf{1}^+$ (R = Ph, X = BF_4, PF_6, or BPh_4; R = Me or CO_2Me, X = PF_6) were isolated as brown air-stable crystalline solids. Alternatively **1** (R = Ph) and iodine yielded the triiodide salt $[Co_2(CO)_2(\mu\text{-}PhC_2Ph)(\mu\text{-}dppm)_2][I_3]$. The synthesis of $[Co_2(CO)_{6-n}(\mu\text{-}RC_2R)\{P(OMe)_3\}_n]^+$ (*n* = 3 or 4, R = Ph or CF_3) from the corresponding neutral complexes and silver(I) salts has been briefly reported.[7]

Each of the new complexes was characterised by elemental analysis (Table 1), IR and ESR spectroscopy, and cyclic voltammetry which showed waves at potentials identical to those for the neutral precursors **1**. The IR spectrum of each cation shows one terminal carbonyl band, shifted to higher wavenumber by *ca.* 50–70 cm^{-1} (*cf.* the neutral complexes). In the case of $\mathbf{1}^+$ (R = CO_2Me) the ketonic carbonyl band is also shifted to higher energy, but to a lesser extent (29 cm^{-1}) than the metal carbonyl band. Similar shifts of the alkyne-substituent absorption were observed[9] on oxidation of $[Mo_2(CO)_4(\mu\text{-}MeCO_2C_2CO_2Me)(\eta\text{-}C_5Me_5)_2]$, shifts which show that the ketonic carbonyl bond order increases with the decrease in back donation from the metals to the alkyne π-acceptor orbitals.

The ESR spectra of complex $\mathbf{1}^+$ are disappointing by comparison to those of the reduced species $[Co_2(CO)_6(\mu\text{-}RC_2R)]^-$ which show extensive hyperfine coupling and which have been fully analysed[6] to provide a detailed description of the LUMO of $[Co_2(CO)_6(\mu\text{-}RC_2R)]$. Each cation shows only one broad line (peak-to-peak separation *ca.* 200 G) at room temperature (g_{iso} = 2.11–2.12) and an even broader (peak-to-peak separation *ca.* 300 G) single-line resonance at 77 K (in a 2:1 thf–CH_2Cl_2 glass) with no resolved hyperfine coupling. Nevertheless, the spectra confirm the paramagnetic nature of $\mathbf{1}^+$ and suggest that the unpaired electron is largely localised on the dimetal centre.

As well as dealing with the structural consequences of removing two electrons from $[Co_2(CO)_6(\mu\text{-}RC_2R)]$ (by forming the diiron analogue) Thorn and Hoffmann's EHMO calculations[1] showed that the LUMO of $[Fe_2(CO)_6(\mu\text{-}RC_2R)]$ was ideally placed to interact with a second alkyne moiety thereby facilitating the synthesis of the well known 'ferrole' complexes $[Fe_2(CO)_6(\mu\text{-}C_4R_4)]$. The chemistry of the cations $\mathbf{1}^+$, in which the equivalent of the LUMO of $[Fe_2(CO)_6(\mu\text{-}RC_2R)]$ is semioccupied, is therefore disappointing; no reaction was observed between $\mathbf{1}^+$ (R = Ph) and PhC_2Ph. The reactivity of $\mathbf{1}^+$ is, in fact, dominated by one-electron reduction to **1** and as such is of little synthetic interest in terms of the activation of the molecule as a whole and the co-ordinated alkyne in particular. The behaviour of $\mathbf{1}^+$ is also in sharp contrast to the reductive chemistry of $[Co_2(CO)_6(\mu\text{-}RC_2R)]$ where the formation of the monoanion (R = CF_3) is the first step in the electron-transfer-chain catalysed substitution by phosphine and phosphite ligands, L, to give $[Co_2(CO)_{6-n}L_n(\mu\text{-}CF_3C_2CF_3)]$ (*n* = 1–3).[11] In addition, less-stable anions (R = Ph, *etc.*) and their P-donor ligand derivatives undergo cleavage in the presence of an excess of L to give novel paramagnetic mononuclear alkyne derivatives such as $[Co(CO)\{P(OEt)_3\}_2(PhC_2Ph)]$.[12]

Although ESR spectroscopy was unhelpful in probing the electronic structure of complex $\mathbf{1}^+$, the successful growth of single crystals of both **1** (R = Me) and $\mathbf{1}^+$ (R = Me) (as its PF_6 salt and dichloromethane solvate) has enabled a comparative X-ray structural analysis to be completed, providing a detailed insight into the nature of the HOMO of **1**. In addition the structure analysis of the phenyl-substituted analogue **1** (R = Ph) as its dichloromethane solvate was carried out for comparison.

X-Ray Structures of $[Co_2(CO)_2(\mu\text{-}PhC_2Ph)(\mu\text{-}dppm)_2]\cdot CH_2Cl_2$, $[Co_2(CO)_2(\mu\text{-}MeC_2Me)(\mu\text{-}dppm)_2]$ *and* $[Co_2(CO)_2(\mu\text{-}MeC_2Me)(\mu\text{-}dppm)_2][PF_6]\cdot CH_2Cl_2$.—The molecular structures of complexes **1** (R = Ph), **1** (R = Me) and $\mathbf{1}^+$ (R = Me) are shown in Figs. 1, 2 and 3. Selected bond lengths and angles for the three structures are given in Tables 2, 3 and 4 respectively. These structures provide the data necessary to monitor both the effect of one-electron oxidation on the geometry of **1** (R = Me) and the effect of phenyl *versus* methyl substitution at the alkyne, as well as the effect of replacement of four carbonyls by the two μ-dppm ligands {by comparison with

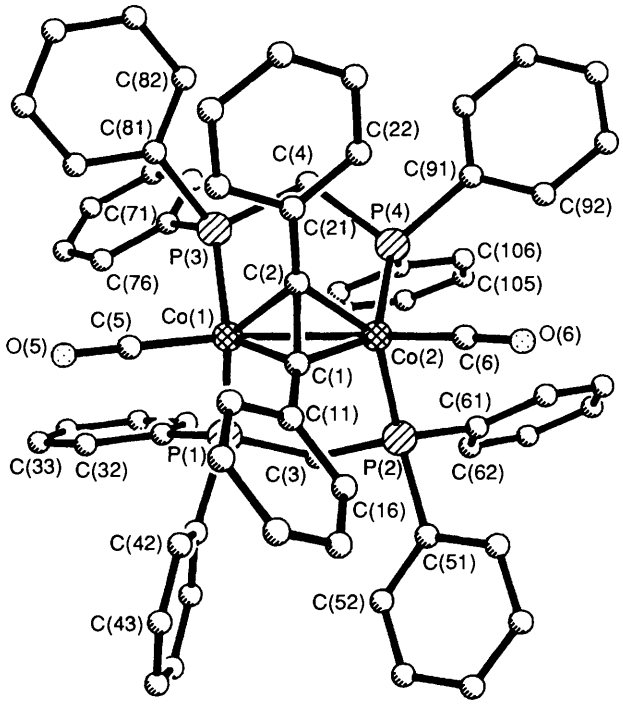

Fig. 1 Molecular structure of complex **1** (R = Ph) showing the atom labelling scheme; all hydrogen atoms have been omitted for clarity

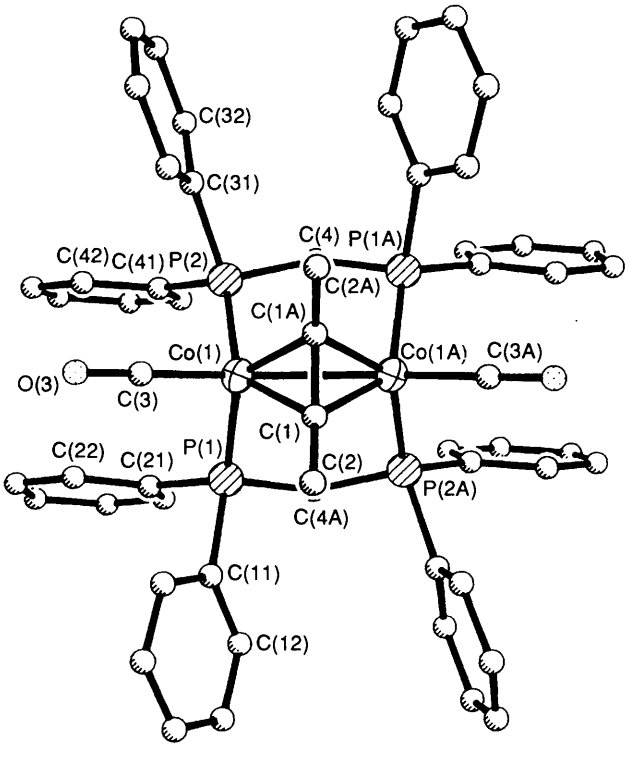

Fig. 2 Molecular structure of complex **1** (R = Me) showing the atom labelling scheme; all hydrogen atoms have been omitted for clarity

the structure of $[Co_2(CO)_6(\mu\text{-}PhC_2Ph)]$ **2**[4]}. The effect of this latter substitution is small on most bond lengths. The Co–Co distance increases on replacement of the carbonyls by dppm, while the average axial Co–C distance is lowered, and the Co–Co–C_{axial} angle is increased [Co–Co 2.508(1) and 2.476(2); Co–C 1.751(4) and 1.804(13) Å; Co–Co–C_{axial} 150.0(1) and 147.9(4)° in **1** (R = Ph) and **2** respectively]. In contrast the cobalt–alkyne and alkyne C–C distances remain essentially constant while the C–C–C_{ipso} angle decreases [Co–C mean

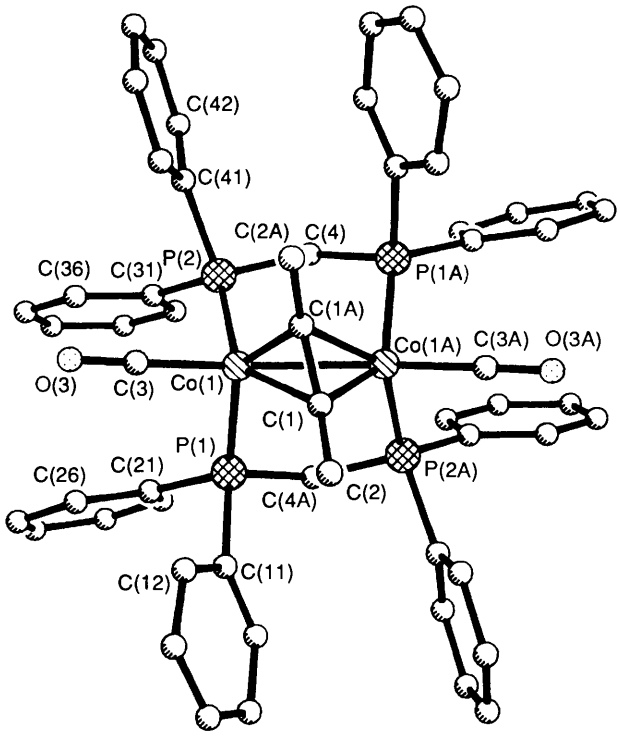

Fig. 3 Molecular structure of complex $\mathbf{1}^+$ (R = Me) showing the atom labelling scheme; all hydrogen atoms have been omitted for clarity

1.963(4) and 1.97(1); C–C 1.360(5) and 1.36(1) Å; C–C–C_{ipso} 135.5(4) and 140.2(9)° in **1** (R = Ph) and **2** respectively]. The effects of replacing Ph by Me are likewise rather small, the most notable being the reduction of the C–C–C_{ipso} angle [to 132.9(2)° in **1** (R = Me)] and the average Co–P bond length [from 2.221(1) in **1** (R = Ph) to 2.203(1) in **1** (R = Me)]. In contrast the effects of one-electron oxidation of **1** (R = Me) are dramatic. The Co–Co bond length is reduced by almost 0.1 Å [from 2.513(1) to 2.418(1) Å], and the alkyne C–C bond in $\mathbf{1}^+$ (R = Me) is twisted by 12.0° relative to the ideal transverse orientation in which it lies at right angles to the metal–metal bond [*cf.* deviations of 0.7 and 0.3° in **1** (R = Me) and **1** (R = Ph)]. The Co–C_{alkyne} bond lengths are distorted as the local geometry of the Co_2C_2 core deviates substantially from C_{2v} symmetry in $\mathbf{1}^+$ (R = Me) to give Co–C 2.103(3) and 1.941(4) Å [*cf.* 1.950(4) and 1.960(3) Å in **1** (R = Me)]. Furthermore there are notable changes in other cobalt–ligand and intraligand bond lengths on oxidation: mean Co–P lengths increase from 2.203(1) to 2.231(1) Å; the Co–CO length increases from 1.750(4) to 1.780(4) Å with corresponding decreases in average P–C and C–O lengths [from 1.839(4) to 1.832(4) and from 1.151(5) to 1.141(5) Å]. The C–C–C_{ipso} angle and the Co–Co–CO_{axial} angle both increase on oxidation [from 132.9(2) to 134.4(2)° and from 150.6(1) to 155.1(1)°]. Perhaps the most unexpected but clearly visible distortion induced by oxidation is on the C_{ipso}–C–C–C_{ipso} torsion angle which is as expected close to zero in **1** (R = Me) and **1** (R = Ph) [2.2(6) and 0.7(6)° respectively] but substantially twisted from the usual *cis* bent geometry typical of transverse μ-alkynes in $\mathbf{1}^+$ (R = Me) at 9.7(6)° (see Figs. 2 and 3).

No structural study of the effects of one-electron transfer on the bonding of alkynes in mononuclear transition-metal complexes has been completed although $[Cr(CO)_2(RC_2R)(\eta\text{-}C_6Me_6)]^{z+}$ (z = 0 or 1; R = Ph or C_6H_4OMe-*p*) were among the first redox pairs to be isolated and characterised[13] spectroscopically. However, the two-electron reduction of $[Fe_3(CO)_9(\mu_3\text{-}RC_2R)]$ to the dianion $[Fe_3(CO)_9(\mu_3\text{-}RC_2R)]^{2-}$ has been shown[14] to lead to a rearrangement in which the bridging alkyne moves from a perpendicular (with respect to

Table 2 Selected bond lengths (Å) and bond angles (°) for complex **1** (R = Ph)·CH_2Cl_2

Co(1)–Co(2)	2.508(1)	Co(1)–P(1)	2.211(1)	Co(2)–P(2)	2.214(1)
Co(1)–P(3)	2.214(1)	Co(2)–P(4)	2.243(1)	P(1)–C(3)	1.847(3)
P(2)–C(3)	1.834(4)	P(3)–C(4)	1.839(3)	P(4)–C(4)	1.841(3)
Co(1)–C(1)	1.972(4)	Co(2)–C(1)	1.949(4)	Co(1)–C(2)	1.974(3)
Co(2)–C(2)	1.958(3)	C(1)–C(2)	1.360(5)	Co(1)–C(5)	1.749(4)
Co(2)–C(6)	1.752(4)	C(5)–O(5)	1.151(5)	C(6)–O(6)	1.153(5)
C(1)–C(11)	1.476(7)	C(2)–C(21)	1.473(4)	P(1)–C(31)	1.843(5)
P(1)–C(41)	1.850(4)	P(2)–C(51)	1.849(5)	P(2)–C(61)	1.843(4)
P(3)–C(71)	1.850(4)	P(3)–C(81)	1.858(3)	P(4)–C(91)	1.844(3)
P(4)–C(101)	1.842(4)	Cl(1)–C(99)	1.502(18)	Cl(2)–C(99)	1.430(15)

Co(2)–Co(1)–P(1)	94.8(1)	Co(2)–Co(1)–P(3)	98.2(1)	Co(2)–P(2)–C(3)	110.3(1)	Co(2)–P(2)–C(51)	121.9(1)
P(1)–Co(1)–P(3)	113.1(1)	C(2)–Co(1)–C(1)	49.8(1)	C(3)–P(2)–C(51)	104.5(2)	Co(2)–P(2)–C(61)	115.5(1)
P(1)–Co(1)–C(1)	107.8(1)	P(3)–Co(1)–C(1)	129.9(1)	C(3)–P(2)–C(61)	103.8(2)	C(51)–P(2)–C(61)	98.9(2)
Co(2)–Co(1)–C(2)	50.1(1)	P(1)–Co(1)–C(2)	141.6(1)	Co(1)–P(3)–C(4)	110.8(1)	Co(1)–P(3)–C(71)	124.8(1)
P(3)–Co(1)–C(2)	90.0(1)	C(1)–Co(1)–C(2)	40.3(1)	C(4)–P(3)–C(71)	106.1(2)	Co(1)–P(3)–C(81)	115.2(1)
Co(2)–Co(1)–C(5)	152.6(2)	P(1)–Co(1)–C(5)	96.6(1)	C(4)–P(3)–C(81)	101.4(1)	C(71)–P(3)–C(81)	95.5(2)
P(3)–Co(1)–C(5)	100.1(1)	C(1)–Co(1)–C(5)	102.8(2)	Co(2)–P(4)–C(4)	108.2(1)	Co(2)–P(4)–C(91)	120.9(2)
C(2)–Co(1)–C(5)	109.6(2)	Co(1)–Co(2)–P(2)	98.9(1)	C(4)–P(4)–C(91)	100.5(1)	Co(2)–P(4)–C(101)	122.9(1)
Co(1)–Co(2)–P(4)	95.9(1)	P(2)–Co(2)–P(4)	101.2(1)	C(4)–P(4)–C(101)	102.1(2)	C(91)–P(4)–C(101)	98.9(2)
Co(1)–Co(2)–C(1)	50.6(1)	P(2)–Co(2)–C(1)	108.7(1)	P(1)–C(3)–P(2)	111.2(2)	P(3)–C(4)–P(4)	115.0(2)
P(4)–Co(2)–C(1)	137.4(1)	Co(1)–Co(2)–C(2)	50.7(1)	Co(1)–C(1)–Co(2)	79.5(2)	Co(1)–C(1)–C(2)	69.9(2)
P(2)–Co(2)–C(2)	144.9(1)	P(4)–Co(2)–C(2)	99.3(1)	Co(2)–C(1)–C(2)	70.0(2)	Co(1)–C(1)–C(11)	135.9(2)
C(1)–Co(2)–C(2)	40.8(1)	Co(1)–Co(2)–C(6)	147.3(1)	Co(2)–C(1)–C(11)	138.1(2)	C(2)–C(1)–C(11)	134.3(3)
P(2)–Co(2)–C(6)	99.1(1)	P(4)–Co(2)–C(6)	107.0(2)	Co(1)–C(2)–Co(2)	79.2(1)	Co(1)–C(2)–C(1)	69.7(2)
C(1)–Co(2)–C(6)	97.6(2)	C(2)–Co(2)–C(6)	101.7(2)	Co(2)–C(2)–C(1)	69.3(2)	Co(1)–C(2)–C(21)	135.7(2)
Co(1)–P(1)–C(3)	113.9(1)	Co(1)–P(1)–C(31)	119.8(1)	Co(2)–C(2)–C(21)	137.3(2)	C(1)–C(2)–C(21)	136.8(4)
C(3)–P(1)–C(31)	102.1(2)	Co(1)–P(1)–C(41)	117.2(1)	Co(1)–C(5)–O(5)	178.7(4)	Co(2)–C(6)–O(6)	174.9(4)
C(3)–P(1)–C(41)	102.6(2)	C(31)–P(1)–C(41)	98.4(2)				

Table 3 Selected bond lengths (Å) and bond angles (°) for complex **1** (R = Me)

Co(1)–Co(1A)	2.513(1)	Co(1)–P(1)	2.209(1)	Co(1)–P(2)	2.197(1)
Co(1)–C(1)	1.950(4)	Co(1)–C(1A)	1.960(3)	C(1)–C(1A)	1.334(8)
C(1)–C(2)	1.508(6)	Co(1)–C(3)	1.750(4)	C(3)–O(3)	1.151(5)
P(1)–C(4A)	1.840(4)	P(2)–C(4)	1.835(4)	P(1)–C(11)	1.835(4)
P(1)–C(21)	1.842(4)	P(2)–C(31)	1.841(5)	P(2)–C(41)	1.836(4)

P(1)–Co(1)–P(2)	104.5(1)	P(1)–Co(1)–C(1)	100.5(1)
P(2)–Co(1)–C(1)	140.6(1)	P(1)–Co(1)–C(3)	101.1(1)
P(2)–Co(1)–C(3)	101.2(2)	C(1)–Co(1)–C(3)	103.2(2)
P(1)–Co(1)–Co(1A)	96.7(1)	P(2)–Co(1)–Co(1A)	96.6(1)
C(1)–Co(1)–Co(1A)	50.2(1)	C(3)–Co(1)–Co(1A)	150.6(1)
P(1)–Co(1)–C(1A)	137.6(1)	P(2)–Co(1)–C(1A)	104.6(1)
C(1)–Co(1)–C(1A)	39.9(2)	C(3)–Co(1)–C(1A)	102.6(2)
Co(1A)–Co(1)–C(1A)	49.8(1)	Co(1)–P(1)–C(11)	116.7(1)
Co(1)–P(1)–C(21)	122.3(2)	C(11)–P(1)–C(21)	98.1(2)
Co(1)–P(1)–C(4A)	110.3(1)	C(11)–P(1)–C(4A)	105.0(2)
C(21)–P(1)–C(4A)	102.1(2)	Co(1)–P(2)–C(4)	112.4(2)
Co(1)–P(2)–C(31)	118.9(1)	C(4)–P(2)–C(31)	102.8(2)
Co(1)–P(2)–C(41)	121.1(1)	C(4)–P(2)–C(41)	101.8(2)
C(31)–P(2)–C(41)	96.9(2)	Co(1)–C(1)–C(2)	136.2(3)
Co(1)–C(1)–Co(1A)	80.0(1)	C(2)–C(1)–Co(1A)	138.3(4)
Co(1)–C(1)–C(1A)	70.5(3)	C(2)–C(1)–C(1A)	132.9(2)
Co(1A)–C(1)–C(1A)	69.6(2)	Co(1)–C(3)–O(3)	177.5(4)
P(2)–C(1)–P(1A)	111.2(2)		

one metal–metal bond) to parallel orientation, a change once again in agreement with MO calculations.[15] Similarly, [(triphos)Rh(μ-Cl)(μ-C_2H_2)Rh(triphos)]$^+$ [triphos = $MeC(CH_2PPh_2)_3$], in which the alkyne is bound orthogonally to the rhodium–rhodium bond, is converted into [(triphos)Rh(μ-Cl)$_2$(μ-C_2H_2)Rh(triphos)]$^{2+}$, in which the alkyne is parallel to the metal–metal bond, by two-electron oxidation in the presence of chloride ion.[16] In the case of **1**$^+$ (R = Me) the dppm ligands constrain the M_2L_6 unit [here $Co_2(CO)_2(\mu\text{-dppm})_2$] to remain close to the eclipsed C_{2v} symmetry observed in 34-electron species such as **1** (R = Me) and **2**. In contrast, without such constraint, 32e species such as [$Fe_2(CO)_6(\mu\text{-}RC_2R)$] show a large distortion of the M_2L_6 unit which renders such complexes less appropriate tests of the theoretical predictions of the consequences of oxidation of the 34e [$M_2L_6(\mu\text{-}RC_2R)$] species. Thorn and Hoffmann suggested[1] that alkyne rotation of *ca.* 20° would be induced in the eclipsed 32e species as a consequence of a second-order Jahn–Teller effect arising from a low-lying vacant orbital of a_2 symmetry interacting with the a_1 HOMO. Using a slightly different computational approach Anderson[2] obtained a rotation of 30°. The observed value of 12° for a one-electron oxidation [*i.e.* for the 33e species **1**$^+$ (R = Me)] is therefore in excellent agreement with these predictions. Furthermore the singly occupied molecular orbital (SOMO) of **1**$^+$ (R = Me) would be expected to be Co–Co π antibonding in character on the basis of Thorn and Hoffmann's work, entirely in accord with the shortening of the Co–Co distance observed on oxidation of **1** (R = Me). The twist in the Me–C–C–Me

Table 4 Selected bond lengths (Å) and bond angles (°) for complex 1^+ (R = Me)PF_6·CH_2Cl_2

Co(1)–Co(1A)	2.418(1)	Co(1)–P(1)	2.243(1)	Co(1)–P(2)	2.219(1)
Co(1)–C(1)	2.103(3)	Co(1)–C(1A)	1.941(4)	C(1)–C(1A)	1.309(8)
C(1)–C(2)	1.506(6)	Co(1)–C(3)	1.780(4)	C(3)–O(3)	1.141(5)
P(1)–C(4A)	1.832(4)	P(2)–C(4)	1.834(3)	P(1)–C(11)	1.827(4)
P(1)–C(21)	1.837(3)	P(2)–C(31)	1.823(4)	P(2)–C(41)	1.839(4)
P–F(1)	1.568(4)	P–F(2)	1.576(3)	P–F(3)	1.582(4)
C(99)–Cl(1)	1.696(18)	C(99)–Cl(2)	1.409(16)		

P(1)–Co(1)–P(2)	101.9(1)	P(1)–Co(1)–C(1)	101.7(1)
P(2)–Co(1)–C(1)	142.7(1)	P(1)–Co(1)–C(3)	100.3(1)
P(2)–Co(1)–C(3)	96.3(1)	C(1)–Co(1)–C(3)	107.3(2)
P(1)–Co(1)–Co(1A)	95.6(1)	P(2)–Co(1)–Co(1A)	99.0(1)
C(1)–Co(1)–Co(1A)	50.3(1)	C(3)–Co(1)–Co(1A)	155.1(1)
P(1)–Co(1)–C(1A)	138.7(1)	P(2)–Co(1)–C(1A)	111.4(1)
C(1)–Co(1)–C(1A)	37.5(2)	C(3)–Co(1)–C(1A)	99.6(2)
Co(1A)–Co(1)–C(1A)	56.4(1)	Co(1)–P(1)–C(11)	112.4(1)
Co(1)–P(1)–C(21)	124.7(2)	C(11)–P(1)–C(21)	98.7(2)
Co(1)–P(1)–C(4A)	109.8(1)	C(11)–P(1)–C(4A)	106.9(2)
C(21)–P(1)–C(4A)	102.8(2)	Co(1)–P(2)–C(4)	110.7(1)
Co(1)–P(2)–C(31)	118.3(1)	C(4)–P(2)–C(31)	105.2(2)
Co(1)–P(2)–C(41)	118.3(1)	C(4)–P(2)–C(41)	102.2(2)
C(31)–P(2)–C(41)	100.2(2)	Co(1)–C(1)–C(2)	140.3(3)
Co(1)–C(1)–Co(1A)	73.3(1)	C(2)–C(1)–Co(1A)	136.6(3)
Co(1)–C(1)–C(1A)	64.5(2)	C(2)–C(1)–Co(1A)	134.4(2)
Co(1A)–C(1)–C(1A)	78.0(2)	Co(1)–C(3)–O(3)	177.7(4)
P(2)–C(4)–P(1A)	110.0(2)		

Table 5 Structure analyses

	1 (R = Ph)·CH_2Cl_2	1 (R = Me)	1^+ (R = Me)PF_6·CH_2Cl_2
Crystal data			
Formula	$C_{67}H_{56}Cl_2Co_2O_2P_4$	$C_{56}H_{50}Co_2O_2P_4$	$C_{57}H_{52}Cl_2Co_2F_6O_2P_5$
M	1205.8	996.7	1226.7
Crystal system	Triclinic	Monoclinic	Monoclinic
Space group (no.)	$P\bar{1}$(no. 2)	$C2/c$ (no. 15)	$C2/c$ (no. 15)
a/Å	17.212(4)	23.476(4)	20.343(3)
b/Å	14.004(3)	9.673(2)	13.834(2)
c/Å	13.416(2)	24.231(8)	20.589(3)
α/°	67.49(2)	90	90
β/°	72.68(2)	116.98(2)	104.98(1)
γ/°	79.50(2)	90	90
U/Å^3	2843(1)	4904(2)	5597(2)
T/K	295	295	295
Z	2	4	4
D_c/g cm^{-3}	1.41	1.35	1.46
F(000)	1244	2064	2508
μ(Mo-Kα)/cm^{-1}	8.3	8.4	8.9
Data collection and reduction			
Crystal dimensions/mm	0.5 × 0.5 × 0.1	0.35 × 0.23 × 0.23	0.62 × 0.42 × 0.28
2θ range/°	4–50	4–50	4–51
Scan method	ω–2θ	ω, Wyckoff	ω, Wyckoff
Scan width, ω/°	1.2 + $\Delta\alpha_1\alpha_2$	1.0	1.0
Total data	8544	4657	5733
Unique data	8297	4203	5203
'Observed' [$F^2 > 1.5\sigma(F^2)$] data N_o	7516	3280	3933
No. azimuthal scan data	396	396	396
Minimum, maximum transmission coefficients	0.734, 0.926	0.799, 0.837	0.541, 0.632
Refinement			
Disordered atoms	None	None	CH_2Cl_2
Least-squares variables, N_v	694	289	348
R*	0.044	0.052	0.050
R'*	0.057	0.050	0.045
S*	1.57	1.33	1.26
g	0.0006	0.000 37	0.0004
Final difference map features/e Å^{-3}	+0.8, −1.0	+0.4, −0.4	+0.45, −0.4

* $R = \Sigma|\Delta|/\Sigma|F_o|$; $R' = (\Sigma w\Delta^2/\Sigma wF_o^2)^{\frac{1}{2}}$; $S = [\Sigma w\Delta^2/(N_o - N_v)]^{\frac{1}{2}}$; $\Delta = F_o - F_c$; $w = [\sigma^2(F_o) + gF_o^2]^{-1}$, $\sigma_c^2(F_o)$ = variance in F_o due to counting statistics.

Table 6 Atomic coordinates ($\times 10^4$) for complex **1** (R = Ph)·CH_2Cl_2

Atom	*x*	*y*	*z*	Atom	*x*	*y*	*z*
Co(1)	2 745(1)	1 764(1)	4 564(1)	C(52)	4 455(3)	4 809(4)	1 530(4)
Co(2)	2 018(1)	3 488(1)	3 749(1)	C(53)	4 981(3)	5 548(4)	1 321(5)
P(1)	3 762(1)	1 936(1)	3 056(1)	C(54)	4 691(3)	6 492(4)	1 344(5)
P(2)	2 901(1)	4 050(1)	2 105(1)	C(55)	3 869(4)	6 718(5)	1 599(6)
P(3)	1 821(1)	762(1)	4 735(1)	C(56)	3 336(3)	5 984(4)	1 825(5)
P(4)	1 094(1)	2 867(1)	3 325(1)	C(61)	2 448(2)	4 703(3)	904(3)
C(3)	3 545(2)	2 957(3)	1 784(3)	C(62)	2 721(3)	4 502(3)	−91(3)
C(4)	909(2)	1 549(3)	4 335(3)	C(63)	2 336(3)	5 022(3)	−949(3)
C(1)	2 604(2)	3 042(3)	4 910(3)	C(64)	1 690(3)	5 733(3)	−835(4)
C(2)	1 886(2)	2 587(2)	5 311(3)	C(65)	1 415(3)	5 926(3)	150(4)
C(5)	3 279(2)	894(3)	5 516(3)	C(66)	1 787(3)	5 418(3)	1 007(3)
C(6)	1 595(2)	4 685(3)	3 876(3)	C(71)	2 023(2)	−271(3)	4 130(3)
O(5)	3 636(2)	338(3)	6 144(3)	C(72)	1 478(3)	−501(4)	3 697(4)
O(6)	1 359(2)	5 466(2)	4 002(3)	C(73)	1 632(3)	−1 350(4)	3 370(5)
C(11)	3 055(2)	3 512(3)	5 364(3)	C(74)	2 323(3)	−1 981(4)	3 463(4)
C(12)	3 144(3)	3 033(3)	6 448(4)	C(75)	2 884(3)	−1 760(3)	3 871(4)
C(13)	3 573(3)	3 476(4)	6 871(4)	C(76)	2 739(2)	−913(3)	4 199(3)
C(14)	3 912(3)	4 390(4)	6 246(5)	C(81)	1 373(2)	−82(3)	6 184(3)
C(15)	3 823(3)	4 880(4)	5 175(5)	C(82)	551(2)	−25(3)	6 722(3)
C(16)	3 402(3)	4 452(3)	4 736(4)	C(83)	243(3)	−700(3)	7 788(3)
C(21)	1 227(2)	2 355(3)	6 346(3)	C(84)	750(3)	−1 426(3)	8 350(3)
C(22)	440(2)	2 821(3)	6 364(3)	C(85)	1 571(3)	−1 493(3)	7 843(4)
C(23)	−174(2)	2 597(3)	7 344(3)	C(86)	1 876(2)	−827(3)	6 769(3)
C(24)	−16(3)	1 903(4)	8 321(4)	C(91)	38(2)	3 464(3)	3 440(3)
C(25)	760(3)	1 421(3)	8 325(3)	C(92)	−124(3)	4 514(3)	3 257(4)
C(26)	1 373(2)	1 638(3)	7 342(3)	C(93)	−910(3)	4 980(4)	3 274(4)
C(31)	4 152(2)	824(3)	2 584(3)	C(94)	−1 542(3)	4 404(4)	3 507(4)
C(32)	4 629(2)	31(3)	3 192(4)	C(95)	−1 395(2)	3 361(4)	3 683(4)
C(33)	4 932(3)	−833(3)	2 898(4)	C(96)	−613(2)	2 894(3)	3 648(4)
C(34)	4 760(3)	−929(4)	2 008(5)	C(101)	1 271(2)	2 680(3)	1 986(3)
C(35)	4 299(3)	−157(4)	1 393(4)	C(102)	1 857(2)	1 922(3)	1 743(3)
C(36)	4 000(3)	724(3)	1 670(4)	C(103)	2 024(3)	1 770(4)	730(4)
C(41)	4 744(2)	2 279(3)	3 077(3)	C(104)	1 611(3)	2 378(4)	−58(4)
C(42)	4 812(2)	2 486(3)	3 968(3)	C(105)	1 035(3)	3 139(4)	160(4)
C(43)	5 536(3)	2 795(4)	3 963(4)	C(106)	859(3)	3 295(3)	1 177(3)
C(44)	6 194(3)	2 899(4)	3 061(5)	Cl(1)	6 819(2)	−110(3)	11 008(2)
C(45)	6 138(3)	2 685(4)	2 168(4)	C(2)	7 751(3)	1 608(4)	9 669(3)
C(46)	5 426(2)	2 371(4)	2 171(4)	C(99)	7 460(13)	656(9)	10 500(22)
C(51)	3 627(2)	5 013(3)	1 791(3)				

backbone was not predicted by these theoretical studies but seems to be consistent with sp^2 hybridisation of the contact carbon atoms and primarily σ-Co–C interaction between the μ-C and the cobalt atom to which it is more tightly bound. Thus the cobalt atom involved in the shorter Co–C vector lies closer to the MeCC plane in $\mathbf{1}^+$ (R = Me) and that in the longer Co–C vector lies further from this plane (displacements of 1.053 and 1.304 Å respectively). The reasons for the significant straightening of the Co–Co–CO axis are also unclear.

Experimental

The preparation, purification and reactions of the complexes described were carried out under an atmosphere of dry nitrogen, using dried, distilled, deoxygenated solvents. Unless stated otherwise (*i*) the complexes were purified by dissolving in CH_2Cl_2, filtering, adding a second solvent (in which the product is insoluble), and reducing the solvent volume *in vacuo* to induce precipitation, and (*ii*) the complexes are air-stable solids which dissolve in polar solvents such as CH_2Cl_2 or tetrahydrofuran (thf) to give moderately air-sensitive solutions. Where necessary the progress of a reaction was monitored by IR spectroscopy.

The compounds $[Co_2(CO)_6(\mu\text{-}PhC_2Ph)]$[17] and $[Co_2(CO)_4(\mu\text{-}RC_2R)(\mu\text{-dppm})]$[18] and the ferrocenium salts $[Fe(\eta\text{-}C_5H_5)_2]X$ (X = PF_6, BF_4 or BPh_4)[19] were prepared by published methods or by modifications thereof.

Electrochemical studies were carried out as previously described.[20] Under the conditions used, E° for the couples $[Fe(\eta\text{-}C_5H_5)_2]^+$–$[Fe(\eta\text{-}C_5H_5)_2]$ and $[Fe(\eta\text{-}C_5Me_5)_2]^+$–$[Fe(\eta\text{-}C_5Me_5)_2]$, used as internal standards, are 0.47 and −0.09 V respectively. The IR spectra were recorded on a Nicolet 5ZDX FT spectrometer, X-band ESR spectra on a Bruker ESP300E spectrometer, and ^1H and ^{31}P NMR spectra on a JEOL FX 90Q spectrometer. Microanalyses were carried out by the staff of the Microanalytical Service of the School of Chemistry, University of Bristol.

Ferrocenium Tetraphenylborate, $[Fe(\eta\text{-}C_5H_5)_2][BPh_4]$.—To a solution of ferrocene (1.0 g, 5.4 mmol) in a mixture of water (20 cm^3) and acetone (8 cm^3) was added anhydrous $FeCl_3$ (1.22 g, 7.5 mmol). After 15 min the deep blue solution was filtered and $NaBPh_4$ (2.57 g, 7.5 mmol) was added. The fine blue precipitate was filtered off, washed with tetrahydrofuran and acetone, and dried, yield 1.01 g (37%). The complex is insoluble in most common solvents and the solid slowly decomposes in air.

Bis[μ-bis(diphenylphosphino)methane]dicarbonyl(μ-diphenylacetylene)dicobalt–Dichloromethane (1:1), $[Co_2(CO)_2(\mu\text{-}PhC_2Ph)(\mu\text{-dppm})_2]\cdot CH_2Cl_2$.—A mixture of $[Co_2(CO)_6(\mu\text{-}PhC_2Ph)]$ (0.47 g, 1.0 mmol) and dppm (0.77 g, 2.0 mmol) in toluene (50 cm^3) was heated under reflux for 16 h. The dark red-brown solution was then cooled and the solvent removed *in vacuo*. The residue was dissolved in the minimum volume of CH_2Cl_2 and placed on an alumina–hexane chromatography column, elution with CH_2Cl_2 giving a red solution which was evaporated to dryness. Purification from CH_2Cl_2–hexane gave the product as a dark purple solid, yield 0.48 g (42%).

Bis[μ-*bis*(*diphenylphosphino*)*methane*]-μ-*but*-2-*yne*-*dicarbonyldicobalt*, $[Co_2(CO)_2(\mu\text{-}MeC_2Me)(\mu\text{-}dppm)_2]$.—A mixture of $[Co_2(CO)_4(\mu\text{-}MeC_2Me)(\mu\text{-}dppm)]$ (0.29 g, 0.43 mmol) and dppm (0.16 g, 0.42 mmol) in toluene (50 cm^3) was heated under reflux for 18 h. The solvent was removed *in vacuo* and the red solid residue was washed with hexane and diethyl ether. Purification from CH_2Cl_2–methanol gave crimson crystals of the product, yield 0.23 g (55%).

The complex $[Co_2(CO)_2(\mu\text{-}MeCO_2C_2CO_2Me)(\mu\text{-}dppm)_2]$ was prepared similarly.

Bis[μ-*bis*(*diphenylphosphino*)*methane*]*dicarbonyl*(μ-*diphenylacetylene*)*dicobalt Hexafluorophosphate*, $[Co_2(CO)_2(\mu\text{-}PhC_2Ph)(\mu\text{-}dppm)_2][PF_6]$.—To a stirred, cooled (0 °C) solution of $[Co_2(CO)_2(\mu\text{-}PhC_2Ph)(\mu\text{-}dppm)_2]$ (0.13 g, 0.12 mmol) in CH_2Cl_2 (30 cm^3) was added $[Fe(\eta\text{-}C_5H_5)_2][PF_6]$ (39 mg, 0.12 mmol). After 5 min the brown solution was filtered and hexane was added to give a brown precipitate. Purification from CH_2Cl_2–diethyl ether gave the product as a brown solid, yield 0.11 g (74%).

The complexes $[Co_2(CO)_2(\mu\text{-}PhC_2Ph)(\mu\text{-}dppm)_2]X$ (X = BF_4 and BPh_4) and $[Co_2(CO)_2(\mu\text{-}RC_2R)(\mu\text{-}dppm)_2][PF_6]$ (R = Me or CO_2Me) were prepared similarly.

Bis[μ-*bis*(*diphenylphosphino*)*methane*]*dicarbonyl*(μ-*diphenylacetylene*)*dicobaltTriiodide*,$[Co_2(CO)_2(\mu\text{-}PhC_2Ph)(\mu\text{-}dppm)_2][I_3]$.—To a stirred, cooled (0 °C) solution of $[Co_2(CO)_2(\mu\text{-}PhC_2Ph)(\mu\text{-}dppm)_2]$ (0.55 g, 0.49 mmol) in CH_2Cl_2 (10 cm^3) was added solid I_2 (0.19 g, 0.75 mmol). After 3 min the purple-brown solution was filtered, evaporated to low volume *in vacuo*, and treated with diethyl ether to give the product as a dark brown solid, yield 0.45 g (61%).

Structure Determinations for Complexes **1** (R = Ph)·CH_2Cl_2, **1** (R = Me) *and* $\mathbf{1}^+$ (R = Me)PF_6·CH_2Cl_2.—Many of the details of the structure analyses carried out on complexes **1** (R = Ph)·CH_2Cl_2, **1** (R = Me) and $\mathbf{1}^+$ (R = Me)PF_6·CH_2Cl_2 are listed in Table 5. X-Ray diffraction measurements were made with Mo-Kα radiation (λ = 0.710 69 Å) using Nicolet four-circle P3m diffractometers on single crystals mounted in thin-walled glass capillaries. Cell dimensions for each analysis were determined from the setting angle values of 15 centred reflections in the range $26 < 2\theta < 30°$.

For each structure analysis intensity data were collected for unique portions of reciprocal space and corrected for Lorentz and polarisation effects, long-term intensity fluctuations, on the basis of the intensities of three check reflections repeatedly measured during data collection, and X-ray absorption on the basis of azimuthal scan data. Only those reflections with prescan counts above a threshold of 15 counts s^{-1} and having $2\theta > 40°$ were measured for **1** (R = Ph)·CH_2Cl_2. The structures were solved by heavy-atom (Patterson and Fourier difference) methods, and refined by blocked-cascade least squares against *F*. For $\mathbf{1}^+$ (R = Me)PF_6·CH_2Cl_2 the dichloromethane solvent showed a two-site disorder about a two-fold axis, all atoms of this molecule being assigned occupancy 0.5. In **1** (R = Me) and $\mathbf{1}^+$ (R = Me)PF_6·CH_2Cl_2 the dicobalt species [as does the anion of $\mathbf{1}^+$ (R = Me)PF_6·CH_2Cl_2] lie at sites of crystallographic two-fold rotational symmetry. All non-

Table 7 Atomic coordinates (× 10^4) for complex **1** (R = Me)

Atom	*x*	*y*	*z*
Co(1)	130(1)	1560(1)	3063(1)
P(1)	1000(1)	276(1)	3389(1)
P(2)	−624(1)	110(1)	2983(1)
C(1)	312(2)	2947(4)	2581(2)
C(2)	795(3)	4088(5)	2715(2)
C(3)	269(2)	2448(4)	3742(2)
O(3)	358(2)	3077(3)	4177(1)
C(4)	−968(2)	−825(4)	2244(2)
C(11)	1765(2)	1199(4)	3675(2)
C(12)	2283(2)	720(6)	3611(3)
C(13)	2860(2)	1428(7)	3864(3)
C(14)	2930(2)	2610(6)	4184(3)
C(15)	2429(2)	3099(6)	4255(3)
C(16)	1849(2)	2410(5)	3996(2)
C(21)	1226(2)	−971(4)	4028(2)
C(22)	1271(3)	−504(5)	4580(2)
C(23)	1452(3)	−1355(7)	5090(2)
C(24)	1598(3)	−2704(8)	5051(3)
C(25)	1535(4)	−3189(7)	4505(4)
C(26)	1347(4)	−2329(6)	3994(3)
C(31)	−1336(2)	788(4)	3026(2)
C(32)	−1832(2)	−73(5)	2973(2)
C(33)	−2353(2)	427(7)	3028(2)
C(34)	−2376(3)	1805(7)	3148(3)
C(35)	−1898(3)	2674(6)	3207(3)
C(36)	−1368(2)	2169(5)	3150(2)
C(41)	−458(2)	−1304(4)	3541(2)
C(42)	−369(3)	−991(6)	4119(2)
C(43)	−245(3)	−1962(6)	4567(3)
C(44)	−218(3)	−3272(6)	4440(3)
C(45)	−301(5)	−3645(6)	3878(3)
C(46)	−416(4)	−2646(5)	3421(3)

Table 8 Atomic coordinates (× 10^4) for complex $\mathbf{1}^+$ (R = Me)PF_6·CH_2Cl_2

Atom	*x*	*y*	*z*	Atom	*x*	*y*	*z*
Co(1)	277(1)	638(1)	3095(1)	C(31)	1231(2)	2668(3)	3738(2)
P(1)	−516(1)	1536(1)	3392(1)	C(32)	1043(2)	3624(3)	3610(2)
P(2)	1083(1)	1720(1)	3101(1)	C(33)	1165(2)	4277(3)	4139(2)
C(1)	−322(2)	−436(3)	2499(2)	C(34)	1463(2)	4009(3)	4783(2)
C(2)	−829(3)	−1210(3)	2542(2)	C(35)	1647(2)	3070(3)	4914(2)
C(3)	681(2)	100(3)	3882(2)	C(36)	1532(2)	2393(3)	4400(2)
O(3)	943(2)	−273(3)	4375(2)	C(41)	1959(2)	1288(3)	3203(2)
C(4)	913(2)	2360(3)	2294(2)	C(42)	2470(2)	1930(3)	3157(2)
C(11)	−1198(2)	803(3)	3566(2)	C(43)	3120(2)	1607(4)	3205(2)
C(12)	−1032(2)	−103(3)	3857(2)	C(44)	3280(2)	656(4)	3307(3)
C(13)	−1512(3)	−688(4)	4038(3)	C(45)	2789(3)	14(4)	3373(3)
C(14)	−2164(3)	−376(4)	3908(3)	C(46)	2124(2)	332(3)	3326(2)
C(15)	−2354(2)	513(5)	3616(3)	P	5000	881(1)	2500
C(16)	−1864(2)	1115(4)	3454(2)	F(1)	5180(2)	1672(2)	2029(2)
C(21)	−353(2)	2326(3)	4134(2)	F(2)	4233(1)	880(2)	2082(2)
C(22)	−485(2)	3308(3)	4102(2)	F(3)	5179(2)	75(2)	2028(2)
C(23)	−411(2)	3843(3)	4684(2)	C(99)	2962(6)	2587(14)	105(7)
C(24)	−196(2)	3418(3)	5301(2)	Cl(1)	2361(4)	3281(4)	314(3)
C(25)	−53(3)	2449(4)	5342(2)	Cl(2)	2978(5)	2754(6)	784(4)
C(26)	−130(2)	1899(3)	4762(2)				

hydrogen atoms were assigned anisotropic displacement parameters and refined without positional constraints. All hydrogen atoms were constrained to ideal geometries (with C–H 0.96 Å) and were assigned fixed isotropic displacement parameters.

Final difference syntheses showed no chemically significant features, the largest being close to the metal, solvent or anion atoms. Refinements converged smoothly to residuals given in Table 5. Tables 6–8 report the positional parameters for these structure determinations. All structure-analysis calculations were made with programs of the SHELXTL[21] system as implemented on a Nicolet R3m/E structure determination system. Complex neutral-atom scattering factors were taken from ref. 22.

Additional material available from the Cambridge Crystallographic Data Centre comprises H-atom coordinates, thermal parameters and remaining bond lengths and angles.

Acknowledgements

We thank the SERC for research studentships (to B. J. D. and P. M. H.), for a postdoctoral research assistantship (to M. C. C.), and for funds to purchase the ESR spectrometer.

References

1 D. L. Thorn and R. Hoffmann, *Inorg. Chem.*, 1978, **17**, 126.
2 A. B. Anderson, *Inorg. Chem.*, 1976, **15**, 2598.
3 F. A. Cotton, J. D. Jamerson and B. R. Stults, *J. Am. Chem. Soc.*, 1976, **98**, 1774.
4 W. G. Sly, *J. Am. Chem. Soc.*, 1959, **81**, 18; D. Gregson and J. A. K. Howard, *Acta Crystallogr., Sect. C*, 1983, **39**, 1024; F. Baert, A. Guelzim and P. Coppens, *Acta Crystallogr., Sect. B*, 1984, **40**, 590.
5 R. P. Aggarwal, N. G. Connelly, M. C. Crespo, B. J. Dunne, P. M. Hopkins and A. G. Orpen, *J. Chem. Soc., Chem. Commun.*, 1989, 33.
6 B. M. Peake, P. H. Rieger, B. H. Robinson and J. Simpson, *J. Am. Chem. Soc.*, 1980, **102**, 156.
7 P. H. Bird, A. R. Fraser and D. N. Hall, *Inorg. Chem.*, 1977, **16**, 1923.
8 M. Arewgoda, P. H. Rieger, B. H. Robinson, J. Simpson and S. J. Visco, *J. Am. Chem. Soc.*, 1982, **104**, 5633; M. Arewgoda, Ph.D. Thesis, University of Auckland, 1981; S. J. Visco, Ph.D. Thesis, University of Auckland, 1982.
9 C. Coates, N. G. Connelly and M. C. Crespo, *J. Chem. Soc., Dalton Trans.*, 1988, 2509.
10 K. Broadley, N. G. Connelly, G. A. Lane and W. E. Geiger, *J. Chem. Soc., Dalton Trans.*, 1986, 373.
11 R. G. Cunninghame, L. R. Hanton, S. D. Jensen, B. H. Robinson and J. Simpson, *Organometallics*, 1987, **6**, 1470; S. D. Jensen, B. H. Robinson and J. Simpson, *Organometallics*, 1987, **6**, 1479; M. Arewgoda, B. H. Robinson and J. Simpson, *J. Am. Chem. Soc.*, 1983, **105**, 1893.
12 J. A. DeGray, Q. Meng and P. H. Rieger, *J. Chem. Soc., Faraday Trans. 1*, 1987, **83**, 3565; L. V. Casagrande, T. Chen, P. H. Rieger, B. H. Robinson, J. Simpson and S. J. Visco, *Inorg. Chem.*, 1984, **23**, 2019.
13 N. G. Connelly and G. A. Johnson, *J. Organomet. Chem.*, 1974, **77**, 341.
14 D. Osella, R. Gobetto, P. Montangero, P. Zanello and A. Cinquantini, *Organometallics*, 1986, **5**, 1247.
15 B. E. R. Schilling and R. Hoffmann, *J. Am. Chem. Soc.*, 1979, **101**, 3456; J.-F. Halet, J.-Y. Saillard, R. Lissillour, M. J. McGlinchey and G. Jaouen, *Inorg. Chem.*, 1985, **24**, 218.
16 C. Bianchini, D. Masi, A. Meli, M. Peruzzini, A. Vacca, F. Laschi and P. Zanello, *Organometallics*, 1991, **10**, 636.
17 R. B. King, *Organomet. Synth.*, 1965, **1**, 133.
18 L. S. Chia, W. R. Cullen, M. Franklin and A. R. Manning, *Inorg. Chem.*, 1975, **14**, 2521; R. S. Dickson and P. J. Fraser, *Adv. Organomet. Chem.*, 1974, **12**, 323.
19 J. C. Smart and B. L. Pinsky, *J. Am. Chem. Soc.*, 1980, **102**, 1009.
20 G. A. Carriedo, N. G. Connelly, M. C. Crespo, I. C. Quarmby, V. Riera and G. H. Worth, *J. Chem. Soc., Dalton Trans.*, 1991, 315.
21 G. M. Sheldrick, SHELXTL 4.1, University of Göttingen, 1985.
22 *International Tables for X-Ray Crystallography*, Kynoch Press, Birmingham, 1974, vol. 4.

Received 13*th September* 1991; *Paper* 1/04759K